Automated lung nodule detection and segmentation

Article *in* Proceedings of SPIE - The International Society for Optical Engineering · February 2009

DOI: 10.1117/12.811985

Martin Fiebich
Technische Hochschule Mittelhessen

Automated lung nodule detection and segmentation

Christian Schneider, Azad Amjadi, Anja Richter, Martin Fiebich*
Institute of Medical Physics and Radiation Protection, University of Applied Sciences Giessen-Friedberg

ABSTRACT

A computer-aided detection (CAD) system for lung nodules in CT scans was developed. For the detection of lung nodules two different methods were applied and only pixels which were detected by both methods are marked as true positives. The first method uses a multi-threshold algorithm, which detect connected regions within the lung that have an intensity between specified threshold values. The second is a multi-scale detection method. The data are searched for points located in spherical objects. The image data were smoothed with a 3D Gaussian filter and computed the Hessian matrix and eigenvectors and eigenvalues for all pixels detected by the first algorithm. By analyzing the eigenvalues points that lie within a spherical structure can be located. For segmentation of the detected nodules an active contour model was used. A two-dimensional active contour with four energy terms describing form and position of the contour in the image data was implemented. In addition balloon energy to get the active contour was used growing out from one point. The result of our detection part is used as input for the segmentation part. To test the detection algorithms we used 19 CT volume data sets from a low-dose CT studies. Our CAD system detected 58% of the nodules with a false-positive rate of 1.38. Additionally we take part at the ANODE09 study whose results will be presented at the SPIE meeting in 2009.

Keywords: Lung, CAD development

1. INTRODUCTION

Lung cancer is the leading cause of cancer deaths in the United States, causing about 160.000 fatalities. In 2008 the American Cancer Society estimates that 29% of all cancer deaths in the United States are due to lung cancer. [1]

Lung Cancer is one of the cancers with the highest mortality, mainly due to the fact of its late detection. Therefore, routine screening programs are considered as a possible option to detect the first signs of the disease in apparently healthy subjects.

Early stage lung cancer is apparent in the form of pulmonary nodules. Smaller nodules (<10 mm diameter) are difficult to detect in x-ray projections, but better visible on CT examinations of the chest. [2] Lung nodules are generally approximately spherical in shape. If they are attached to the chest wall or to vessels, their forms are in the range of spherical to hemispherical. On CT images lung nodules appear as circular shaped brighter areas, with grey-values very similar to those of blood vessels in the lungs.

Even with better visibility on CT examinations, diagnosis of these studies is a time-consuming and error-prone task for a radiologist. Studies have shown that radiologists frequently fail to detect all visible nodules in a scan. [3, 4] The sensitivity of radiologists for detection of pulmonary nodules $\leq$ 5 mm was < 70 % and < 95 % for nodules > 5 mm. [5, 6] Therefore computer-assisted detection (CAD) solutions for lung nodule detection on CT scans have been developed.

The previous developed method uses a multi-threshold algorithm and a rule-based classification scheme. This method has the lack of a low sensitivity and has problems with nodules attached to the pleural wall. [7, 8] Therefore an addition detection scheme was implemented and active contours for the segmentation were used.

* Martin.Fiebich@tg.fh-giessen.de

Medical Imaging 2009: Computer-Aided Diagnosis, edited by Nico Karssemeijer, Maryellen L. Giger
Proc. of SPIE Vol. 7260, 72601T · © 2009 SPIE · CCC code: 1605-7422/09/$18 · doi: 10.1117/12.811985

2. METHODS AND MATERIALS

A CAD system was developed, named IMPSCad, which implements the algorithms described in this work. The graphical user interface (GUI) is shown in figure one. On the upper left side there is the actual slice displayed and after segmentation and detection there will be shown the results with different colors. On the upper right side is a maximum intensity projection (MIP). At the bottom left corner a region of interest is displayed which can be set by the user. The rest is for winding, status information and settings.

The system works as follows. After the image data are loaded into the system, a median filter is applied on the image data to reduce noise in the image data. Then the contour of the chest is detected by a chain-code algorithm. With this information it is possible to eliminate the surrounding data which is not necessary for the following parts and would only increase further computation time. In addition for chest segmentation a 3D region growing to eliminate all structures which don’t belong to the lungs is used. Bigger vessels connected to the heart will be eliminated in this step. The algorithm starts in the middle of the data set growing through all slices. The detected data are not used in further process because we are only interested in nodules placed in the lung. All the blood vessels reaching into the lung would disturb our detection algorithm rather lead to an increased number of false positives.

After this step two different algorithms are used, which are described in detail on the next pages, to detect nodules in the lungs. After the detection of the center position of possible nodule candidates the segmentation is started. For this purpose the active contour model introduced by Kass et al. [9] is used. Details of this model will be explained in part 2.3.

Fig. 3: User interface of IMPSCad

2.1 Chain-Code

In this part the chain code algorithm will be described, which is used for chest contour detection. This algorithm is used to describe an object by unit size line segments with a given orientation. Based on a starting point the algorithm follows the contour of the object, in our case the chest. All the possible directions where the next pixel of the contour could be located are described by indices i.e. '0' – top, '1' – right, '2' – bottom, '3' – left for a four pixel neighborhood. This is visualized for an eight pixel neighborhood in figure two. The algorithm saves the direction of the contour and steps to the detected pixel. From there it starts searching for a possible contour pixel again. This is repeated until the algorithm gets back to the starting point. The result is a given start location and a list of direction indices by which the contour of the object is described. Figure three illustrates an example contour extraction.

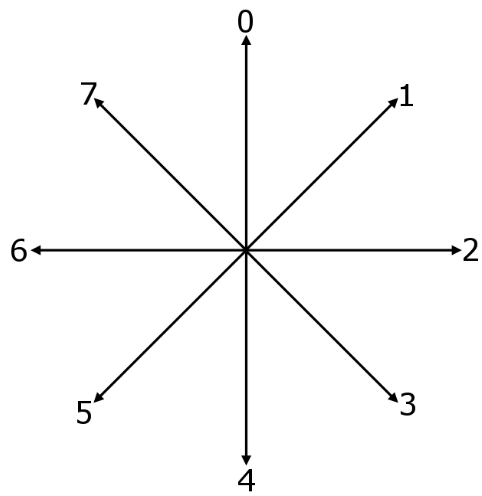

Fig. 2: Example for an eight pixel neighborhood relation described by the indices of the chain code algorithm

As one can see this algorithm is only capable for closed contours, like in our case the contour of the chest. Also the user has to define a threshold to distinguish between the object and background. The starting point, which is needed for this algorithm, could be located by searching from the upper left corner of the picture for the first pixel of the object whose left neighbor belongs to the background of the image.

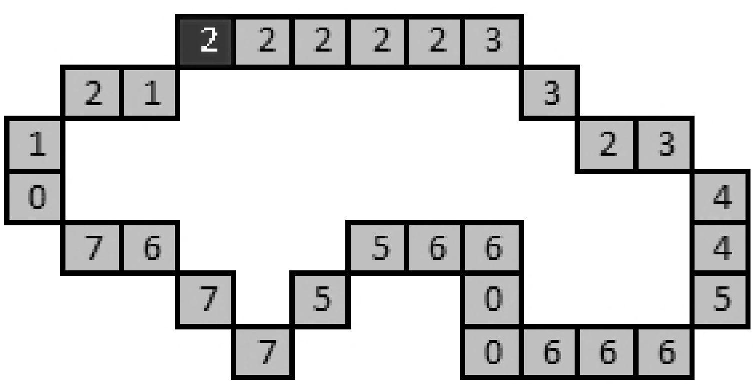

Fig. 3: Example for an object contour extracted with a chain code algorithm. The black lodged box shows the starting point and the numbers in the small boxes represent the direction indices.

2.2 Detection Algorithm

The results of two algorithms are used for detecting lung nodules which will be described in this part. The first method depends on the work of Fiebich et al. [1]. It is a grayscale threshold method which analyses the complete lung. It searches for voxel in the lung which have a grayscale value between two defined thresholds. If the grayscale of a voxel is between the threshold the voxel is marked by the algorithm and a 3D region growing with an eight neighbor relation is started, first with a low and then with a high threshold. These regions are marked for further processing and analysis.

The second method is a multi-scale algorithm which is described by Krissan et al. [10] and was used to locate and display cylindrical vessels. We modified this algorithm for detection of lung nodules in our CAD scheme. It detects structures by using Hessian matrix and eigenvalues. For this it analyses the eigenvalues of the Hessian matrix of all volume elements to suggest if there is a local spherical structure present.

This algorithm is used because the structures we want to detect with our CAD system are spherical, have diameters between 2 mm and 30 mm and have a higher intensity in relation to the background. The intensity of each pixel is defined as $I(x)$. $\nabla I(x) = 0$ is true for points with maximum intensity. The Taylor series for I at $x + hv$ is $I(x+hv) = I(x) + h\nabla I(x) \cdot v + \frac{1}{2}h^2 v^T \cdot H(I)v + \varepsilon$. The direction of this Taylor series is given by vector v, whereas $\|v\| = 1$ and h equates the size of the Gaussian filter kernel. The kernel of the Gaussian filter is proportional to the diameter of structures detected by the system. With a nearly small remainder term ε, the variation of intensity is only dependent from the term $v^T H(I)v$. This term gets its highest value if v is an Eigenvector of the Hesse matrix $H(I)$ [2]. Those eigenvectors build a three-dimensional vector space, with one vector pointing in the direction of highest intensity change. Orthogonal to this vector are the two other vectors arranged. The eigenvalues correspond to the length of the eigenvectors and are a measurement for change of intensity in the corresponding direction. From this it follows that eigenvectors with similar length show the existence of a spherical structure.

To detect structures, different in diameter, the data set is convolved with stepwise enlarged Gaussian kernel. Also for each voxel, marked by the first algorithm, the Hesse matrix and its eigenvalues are computed following a comparison of the eigenvalues. This is only done for the voxel marked by the first algorithm because we would only mark a voxel as a nodule candidate, if it is detected by both methods. So by computing the Hesse matrix and its eigenvalues only for the marked pixel, needs less computation time than letting this algorithm work without the input of the first one. After this all voxels with similar eigenvalues are marked as voxels of nodule candidates.

2.3 Active contour segmentation

In addition to this detection functionality there is a segmentation part implemented which could be used to extract the detected nodules. For this the active contour model, also called snake, introduced by Kass et al. [9] is used. An example image with the result of an active contour segmentation is shown in figure five. As input fot the segmentation part the results of the detection part are used. Every detected nodule will be segmented. For this a region of interest (ROI) surrounding a nodule is extracted. This ROI is about 50 pixels in length and 50 pixels in height.

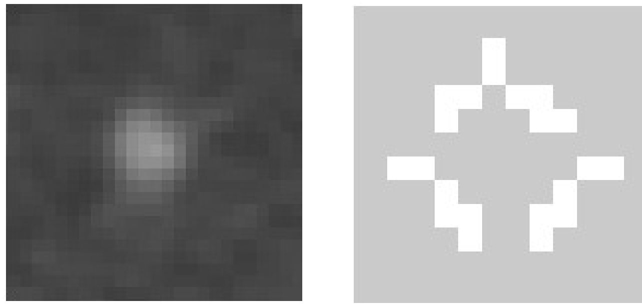

Fig. 4: Example for the canny edge detection. On the left side one can see the original picture including a nodule an on the right side the result of an canny edge detection. Note that the picture on the right is zoomed in and so has not the same dimension like the original on the right.

In the next step the canny edge detection operator is used to extract edges in the ROI. It was developed by John Canny for ideal edge detection. This algorithm might be more complex than other edge detection algorithms but therefore it has advantages in computation time. In figure four one can see a sample of such a ROI and a zoomed picture with the result of the canny edge detection operator applied to a sample picture.

It can be seen that the extracted border has gaps. Because of this, extracting nodules with use of a simple region growing algorithm is not possible. The region growing algorithm would leave the structure through the gaps and thus leading to an incorrect segmentation of the candidate. This is the part where the active contour model is used.

Snakes are energy minimizing splines. The contour is represented as a vector $\mathrm{v(s)} = (\mathrm{x(s)}, \mathrm{y(s)})$ with s being arc length. The quality of the actual status is given by the total energy

$$\mathrm{E}^*_{\mathrm{Snake}} = \int_0^1 E_{Snake}(v(s))ds$$

of the snake. The better the status of the snake the lower is the result of the energy. Thus if the snake gets nearer to the contour that should be extracted, the energy gets lower. The energy of the snake is given by several energy terms

$$\mathrm{E}^*_{\mathrm{Snake}} = \int_0^1 E_{\mathrm{int}}(v(s)) + E_{image}(v(s)) + E_{bal}(v(s))ds$$

which describe different aspects of the snake.

E_{int} represents the internal energy of the contour due to bending or discontinuities. It is given by the term

$$\mathrm{E}_{\mathrm{int}} = \frac{1}{2}(\alpha(s)\, E_{continuity} + \beta(s)\, E_{curvature})$$

where

$$\mathrm{E}_{\mathrm{continuity}} = \left|v_S(s)\right|^2$$

will let the snake act like a membrane and

$$\mathrm{E}_{\mathrm{curvature}} = \left|v_{SS}(s)\right|^2$$

will let it act like a thin plate. Each of them has a factor to control the influence of these terms. These factors are set constant for the whole snake. To use the energy in a discrete system, the snake is approximated by finite differences. That leads to

$$E_{\text{continuity}} \approx \left|v_i - v_{i-1}\right|^2$$

$$E_{\text{curvature}} \approx \left|v_{i-1} - 2v_i + v_{i+1}\right|^2$$

D. J. Williams et al. [12] determined that the term for continuity estimation leads to shrink the snake. They proposed to use

$$E_{\text{continuity}} \approx \overline{d}\left|v_i - v_{i-1}\right|^2$$

where $\overline{d}$ is the mean distance between all points of the snake. This leads to low energy if the points of the snake move within the mean distance.

E_{image} is the image force which attracts the contour to edges in the image. Cohen et al. [11] proposed to use the result of a canny edge detection algorithm as input of the image force. The result of this canny algorithm is a image $I_{\text{Canny}}(x, y)$ which consists of the edges of the contour which should be extracted. The equation of this image energy is

$$E_{image} = -\gamma(s)\left|I_{Canny}(x, y)\right|$$

A negative factor is used because the edges are described by positive values in the resulting image of the canny algorithm. Like the factor of the continuity and curvature energy this is set as constant for the whole snake.

The last energy term E_{bal} is a balloon force, introduced by Cohen et al. [11]. This force has the same effect to the contour like air blew into a balloon. The equation for this energy is

$$E_{bal} = \delta(n(c) \cdot (v'(c) - v(c)))$$

where $n(c)$ is the normal vector of the curve and $v'(c)$ the new position where $v(c)$ moves to. The smaller the angle between normal vector of the curve and new position of the point, the higher is the value of the balloon energy. Because of this a negative factor δ is chosen to get the snake expanding. If you want a shrinking snake you have to choose a positive factor. The balloon force is essential for our system because without this force the initial snake has to be placed near to the contour that should be extracted. Otherwise the snake would not be attracted to the contour which is searched. So with the balloon force it is possible to initialize the snake inside of the object which should be extracted. This starting point is a result of the detection algorithm which marks pixel in the center of a nodule.

To get the snake to the contour of the nodule which should be extracted, the energy of the snake has to be minimzed. This energy minimization is done by a Greedy algorithm. The greedy algorithm is an iterative one. To minimize the energy of the snake, the energy of every point of the snake is minimized. This is done by calculating the energy for every possible new position of a point and moving it to the position with the lowest energy. This is repeated until the algorithm reaches a maximum number of iterations or it doesn't find any new position where the energy of the snake is lower.

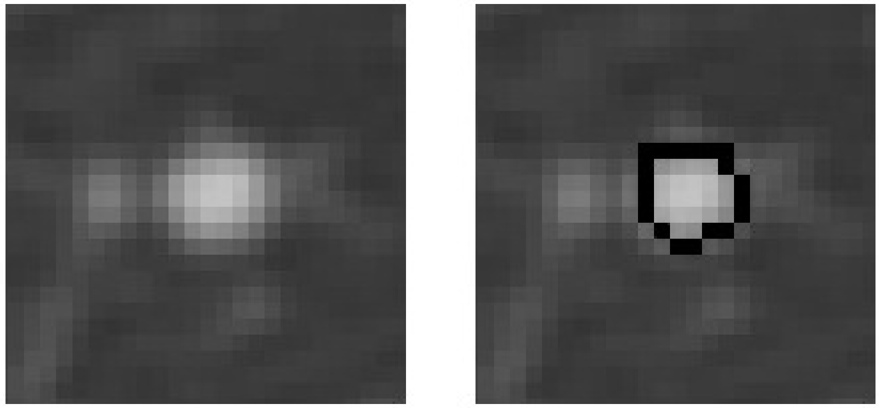

Fig. 5: This figure illustrates the result of the active contour segmentation task. On the left side the one can see the ROI including a nodule and on the right side the contour which was extracted by the algorithm

2.4 Data sets

We used 19 CT volume data sets from a Siemens low dose study with 191 lung nodules. The CT scans were acquired with either Siemens Sensation 16 or Siemens Volume Zoom. The data sets consist of average 393 images. The size of each image is 512 x 512 pixels. Slice thickness varies between 0.44 and 0.78 mm. The data was analyzed by three radiologists and one CAD system. Additionally we participated in ANODE09 study organized by van Ginneken (Image Sciences Institute, University Medical Center Utrecht), Prokop (Department of Radiology, University Medical Center Utrecht) and Armato III (Department of Radiology, The University of Chicago). The goal of the study is to compare the various methods available for automatic detection of pulmonary nodules in thoracic CT scans. Therefore they provided five example scans to train algorithms, and 50 test scans for comparing the algorithms. The results of this study will be presented at the SPIE Medical Imaging 2009.

3. RESULTS

Our CAD system detected 58% of the nodules within the Siemens data sets with a false-positive rate of 1.38. Computation time for a whole study was less than five minutes. The results of our system with the data of the ANODE09 study will be presented at the SPIE Medical Imaging Conference 2009. The results from the automatic nodule extraction with active contours are also good.

4. CONCLUSION

The analysis of local structures with Eigenvectors like our multiscale algorithm is a robust, high sensitive technique which is, in combination with other algorithms, a very good method for nodule detection. The specificity of this technique depends on the adjusted sensitivity. The result of the automatic segmentation of lung nodules depends on the chosen start point and the size of the nodule. Additional to the used energy terms there could be introduced some other terms which, maybe, use three-dimensional information.

REFERENCES

[1] American Cancer Society, "Cancer facts and figures", 2008.

[2] C. Henschke, D. I. McCauley, D. F. Yankelevitz, D. P. Naidich, G. McGuinness, O. S. Miettinen, D. M. Libby, M. Pasmantier, J. Koizumi, N. K. Altorki, and J. P. Smith, "Early Lung Cancer Action Project: Overall design and findings from baseline screening," *The Lancet* **354**, pp. 99–105, 1999.

[3] R. Kakinuma, H. Ohmatsu, M. Kaneko, K. Eguchi, T. Naruke, K. Nagai, Y. Nishiwaki, A. Suzuki, and N. Moriyama, "Detection failures in spiral CT screening for lung cancer: Analysis of CT findings," *Radiology* **212**, pp. 61–66, 1999.

[4] J. Gurney, "Missed lung cancer at CT: Imaging findings in nine patients," *Radiology* **199**, pp. 117–122, 1996.

[5] S. E. Seltzer, P. F. Judy, U. Feldman, L. Scarff, F. L. Jacobson, "Influence of CT image size and format on accuracy of lung nodule detection," *Radiology* **206**, pp. 617-622, 1998

[6] S. Diederich, M. Semik, M. G. Lentschig, F. Winter, H. H. Scheld, N. Roos, G. Bongartz, "Helical CT of pulmonary nodules in patients with extrathoracic malignancy: CT-surgical correlation," *AJR Am J Roentgenol.* 1999 Feb;172(2):353-60.

[7] M. Fiebich, D. Wormanns, W. Heindel, "Improvement of method for computer-assisted detection of pulmonary nodules in CT of the chest," *SPIE Proceedings* **4322**, *Medical Imaging 2001*: Image Processing, M. Sonka, K. M. Hanson, Editors, pp. 702-709, 2001

[8] D. Wormanns, M. Fiebich, M. Saidi, S. Diederich, W. Heindel, "Automatic detection of pulmonary nodules at spiral CT: clinical application of a computer aided diagnosis system," *Eur Radiol* **12**, pp. 1052-1057, 2002

[9] M. Kass, A. Witkin, D. Terzopoulos, "Snakes: active contours models," In: Proceedings of the First International Conference on Computer Vision, *ICCV 1987*, pp. 259-268, 1987

[10] K. Krissian, G. Malandain, N. Ayache, "Model Based Multiscale Detection and Reconstruction of 3D Vessels" **Inria**, Institut National de Recherche en Informatique et en Automatique. (RR-**3442**). – Technical Report,1998

[11] L. D. Cohen, I. Cohen, "Finite element methods for active contour models and balloons for 2-D and 3-D images," *IEEE Transactions on Pattern Analysis and Machine Intelligence*, PAMI-15, **11**, pp. 1131-1147, 1993

[12] D. J. Williams, M. Shah, "A fast algorithm for active contours and curvature estimation," *Computer Vision Graphics and Image Processing* CVGIP: Image Understanding **55**(1), pp. 14-26, 1992